ELSEVIER

Journal of Nuclear Materials 273 (1999) 95–101

journal of nuclear materials

www.elsevier.nl/locate/jnucmat

Relationship between hardening and damage structure in austenitic stainless steel 316LN irradiated at low temperature in the HFIR

N. Hashimoto [a,*], E. Wakai [b], J.P. Robertson [a]

[a] *Metals and Ceramics Division, Oak Ridge National Laboratory (ORNL), P.O. Box 2008, Oak Ridge, TN 37831-6376, USA*
[b] *Japan Atomic Energy Research Institute, Tokai-mura, Ibaraki-ken 319-11, Japan*

Received 6 October 1998; accepted 9 December 1998

Abstract

An austenitic stainless steel 316LN irradiated to damage levels of about 3 dpa at irradiation temperatures of about 90°C and 250°C has been examined by transmission electron microscopy. The irradiation at 90°C and 250°C induced a dislocation loop density of 3.5×10^{22} and 5.2×10^{22} m^{-3}, and a black dot density of 2.2×10^{23} and 1.1×10^{23} m^{-3}, respectively, in the steel. A low density ($<1 \times 10^{19}$ m^{-3}) of radiation-enhanced precipitates was observed in the matrix. No cavities were observed. These features are correlated with the changes in tensile properties. It is concluded that the dislocation loops and the black dots cause irradiation hardening and a decrease in the uniform elongation in the 316LN steel irradiated at low temperatures.

PACS: 61.72

1. Introduction

An austenitic stainless steel, 316LN is the first wall and shielding structural material proposed for the International Thermonuclear Experimental Reactor (ITER) [1]. The proposed operational temperature range for the structure is 100–250°C, which is below the temperature regimes for void swelling and for grain boundary embrittlement. For austenitic stainless steels, neutron irradiation at these temperatures increases the yield strength and decreases the uniform elongation and lowers the fracture toughness. As reported earlier, the magnitude of these changes is both temperature and dose dependent [2–4].

The objective of this study is to investigate the microstructure of 316LN austenitic stainless steel irradiated at low temperatures up to 3 dpa in order to relate the changes in mechanical properties to the microstructure.

2. Experimental procedure

The chemical composition of the 316LN used in this study falls within the specifications for the ITER reference grade material (316LN-IG), as shown in Table 1. Standard 3-mm diameter transmission electron microscopy (TEM) disks were punched from 0.25-mm thick sheet stock, and then these disks were solution annealed. They were irradiated in the High Flux Isotope Reactor (HFIR) in the capsules HFIR-MFE-JP-17 and -JP-18 to neutron fluences producing 3 dpa. The exposures for the JP-17 and JP-18 were 3702 MWd, or approximately 43.6 days at 85 MW reactor power, and the capsule achieved a peak fluence of 3 dpa. These capsules were designed for irradiation temperatures of either 60–125°C (nominally 90°C) or 250–300°C (nominally 250°C) [5–7]. The calculated helium concentration generated as a result of transmutation of nickel was about 65 appm; this is about a factor of two higher than that expected for the ITER first wall blanket and shield structure after a neutron exposure that would produce 3 dpa.

The TEM specimens were thinned using an automatic Tenupol electropolishing unit in a shielded glove

* Corresponding author. Tel.: +1-423 576 2714; fax: +1-423 574 0641; e-mail: hashimoton@ornl.gov

0022-3115/99/$ – see front matter
PII: S0022-3115(99)00009-4

Table 1
Chemical compositions of 316LN and 316LN-IG (wt%)

Steel	Fe	Cr	Ni	Mo	Mn	Si	C	N
316LN	Bal.	17.4	12.3	2.3	1.8	0.46	0.024	0.06
316LN-IG (min)	Bal.	17.0	12.0	2.3	1.6	0.50	0.015	0.06
316LN-IG (max)		18.0	12.5	2.7	2.0		0.030	0.08

box. TEM disks were examined using a JEM-2000FX transmission electron microscope. The foil thicknesses (~100 nm) were measured by thickness fringes, which appear to be black or white depending on the thickness of the specimen, in order to quantify defect density values.

3. Results

3.1. Dislocations and dislocation loops

Fig. 1 shows dislocations or dislocation loops in 316LN before and after irradiation up to 3 dpa. The electron micrographs were taken with beam direction **B** close to [0 1 1]. Fig. 1(a) is a dark-field image in the unirradiated specimen, and Fig. 1(b) and (c) are dark-field images in the specimens irradiated at 90°C and 250°C, which are taken using streaks in the diffraction pattern arising from the faulted loops. The loops observed in specimens irradiated at 90°C or 250°C were Frank type faulted loops on {1 1 1} planes, which were identified by reflection from stacking faults in weak-beam dark-field image. The irradiation at 250°C induced a slightly higher dislocation loop density compared with the irradiation at 90°C. The line density, i.e. the faulted loop line length per unit volume, is 1.4×10^{15} m^{-2} after the irradiation at 250°C, which is about twice as high as the faulted loop line length observed after the 90°C irradiation. The dislocation density in the unirradiated specimen and the faulted loop densities and sizes of the irradiated specimens are shown in Table 2.

Irradiation at either temperature also induced small defect clusters (black dots) in the matrix, Table 2 and Fig. 2. These images were obtained on the diffraction conditions: $\mathbf{B} \approx [0\ 1\ 1]$, $\mathbf{g} = 200$, ($\mathbf{g}$, $6\mathbf{g}$). The number density and the mean diameter of black dots at 90°C and 250°C were 2.2×10^{23} m^{-3} and 1.2 nm, and 1.1×10^{23} m^{-3} and 1.2 nm, respectively. In the present work, the black dot density and the mean diameter were measured in relatively thin foils ($t \approx 100$ nm).

Fig. 3 shows another dark-field image in the specimen irradiated at 250°C, which was obtained on the diffraction conditions: $\mathbf{B} \approx [0\ 0\ 1]$, $\mathbf{g} = 200$, ($\mathbf{g}$, $5\mathbf{g}$). The defects observed as edge-on loops were unfaulted dislocation loops on {1 1 0} planes. The loops on {1 1 0} planes were observed only in the specimen irradiated at 250°C. The number densities and the mean diameter of these loops were 1.2×10^{21} m^{-3} and 10 nm, respectively.

3.2. Precipitate evolution

As shown in Fig. 4, precipitates were observed in the matrix irradiated at 90°C and 250°C but not on grain boundaries. They were identified as $M_{23}C_6$ carbides from the spacing of the Moiré fringes. The measured

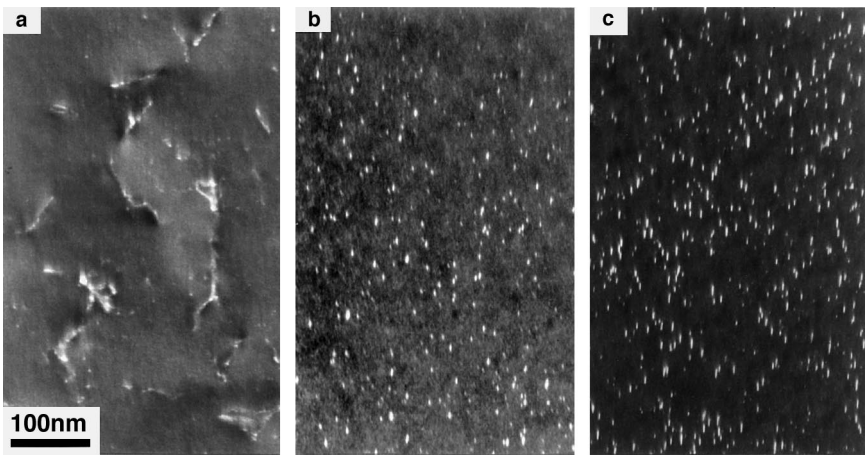

Fig. 1. Dislocations or dislocation loops in 316LN before and after HFIR irradiation up to 3 dpa. Micrographs were taken with beam direction **B** close to ⟨1 1 0⟩. (a) is a dark-field image in the unirradiated specimen, (b) and (c) are dark-field images taken using streaks arising from faulted loops in the specimens irradiated at 90°C and 250°C.

Table 2
Summary of dislocation, dislocation loop, and black dot density of 316LN irradiated to 3 dpa (the average thickness of the measured area is less than 100 nm)

Condition	Black dot		Faulted loop		Unfaulted loop on {1 1 0}		Total line density (m^{-2})
	Number density (m^{-3})	Mean diameter (nm)	Number density (m^{-3})	Mean diameter (nm)	Number density (m^{-3})	Mean diameter (nm)	
Before irradiation	–	–	–	–	–	–	1×10^{14}
Irr. at 90°C	2.2×10^{23}	1.2	3.5×10^{22}	7.6	–	–	8.3×10^{14}
Irr. at 250°C	1.1×10^{23}	1.2	5.5×10^{22}	8.0	1.2×10^{21}	10	1.4×10^{15}

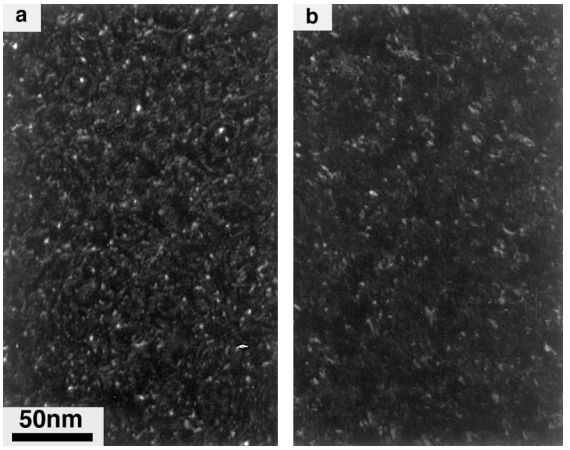

Fig. 2. Black dot defects in 316LN after HFIR irradiation up to 3 dpa. The micrographs are dark-field images in the specimens irradiated at: (a) 90°C and (b) 250°C. The average foil thickness is about 100 nm.

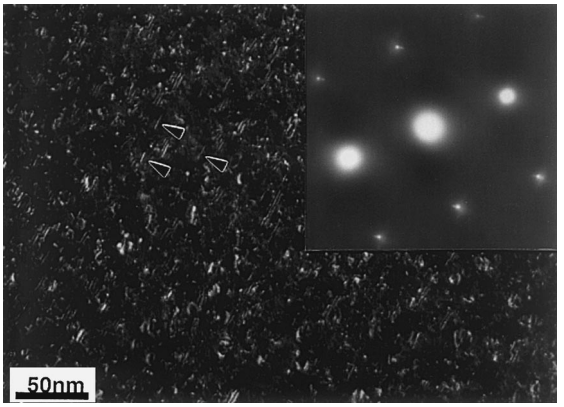

Fig. 3. Dark-field image formed using a streak observed in the diffraction pattern in the specimen irradiated at 250°C in HFIR. Loops on {1 1 0} are observed.

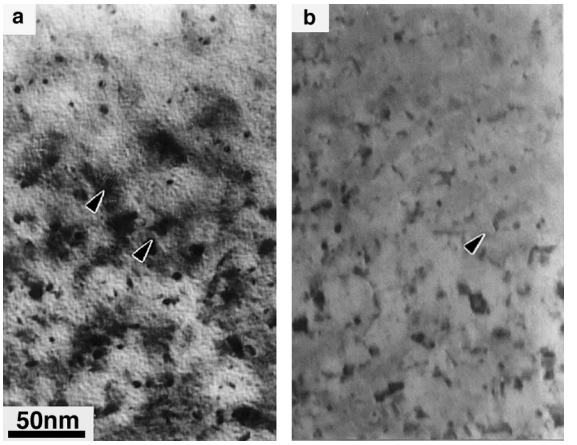

Fig. 4. $M_{23}C_6$ carbides in 316LN after HFIR irradiation up to 3 dpa. The micrographs are bright-field images in the specimens irradiated at: (a) 90°C and (b) 250°C.

spacings (1.5 and 1.7 nm) correspond to the spacing of the Moiré fringes of $M_{23}C_6$ for $\mathbf{g} = 200$, which were identified as {1 1 5} and {5 3 3} planes in $M_{23}C_6$, respectively. The number density and the mean diameter of $M_{23}C_6$ at 90°C and 250°C are nearly equal, and the values are less than 1×10^{19} m^{-3} and 14 nm, respectively. There is no clear difference in the precipitate densities between irradiation temperatures. These data are summarized in Table 3.

Table 3
Precipitate $M_{23}C_6$ in 316LN before and after irradiation to 3 dpa at 90°C and 250°C

Condition	Number density (m^{-3})	Mean diameter (nm)
Before irradiation	–	–
Irr. at 90°C	$<1 \times 10^{19}$	13
Irr. at 250°C	$<1 \times 10^{19}$	14

4. Discussion

4.1. Microstructures

HFIR irradiation up to 3 dpa induced faulted dislocation loops. The faulted loops formed at 90°C and 250°C were identified as Frank type loops lying on {1 1 1} planes with Burgers vectors of type $\mathbf{b} = (1/3)\mathbf{a}_0$ ⟨1 1 1⟩. The dislocation loop density at 250°C is slightly higher than that at 90°C. Previous studies have shown that both the nature and number density of defects formed in type 316 austenitic stainless steel during neutron irradiation is strongly dependent on irradiation temperature [8–10]. Corbett et al. [11,12] characterized a low temperature regime as extending from the onset of vacancy motion up to the temperature where vacancy clusters created in the displacement cascade become thermally unstable. The current study is within this low temperature regime. The number densities of faulted Frank loops reported here are consistent with the values reported by Maziasz for irradiation at 60°C to 1–2 dpa [13] and by Tanaka for irradiation at 300°C to 10 dpa [14] or Horiki for low irradiation dose at 300°C [15].

At these low temperatures, the total dislocation density is dominated by faulted loops [16,17], and the total dislocation densities were calculated from the dislocation loop density and the mean diameter as 8.3×10^{14} and 1.4×10^{15} m^{-2} at 90°C and 250°C, respectively. These values are consistent with the results of previous analyses of austenitic stainless steels irradiated in the HFIR [18].

In other work at higher irradiation temperatures (>450°C), Frank loops tend to unfault to form the perfect loop configuration with $\mathbf{b} = (1/2)\mathbf{a}_0$ ⟨1 1 0⟩ Burgers vectors, which can glide to interact and form network dislocations [8]. In the present experiment, unfaulted dislocation loops on {1 1 0} planes with mean size of ≈10 nm were observed after irradiation at 250°C. It seems that there is sufficient probability for the unfaulting reaction at 250°C, which can be triggered by physical impingement of adjoining Frank loops as a result of loop growth [19], because a distance between segments of loops is small due to high number density and large mean size. About 4% of the Frank loop population were converted.

The irradiation also induced small defect clusters (black dots) in the matrix. The visibility of very small clusters depends on the foil thickness, with the visible cluster density in very thin foils being higher than that found in thick foils [20]. In the present work, the black dot density and the mean diameter were measured in relatively thin foils ($t \approx 100$ nm). The small defect clusters are probably dislocation loops and/or stacking fault tetrahedra (SFT) [15], but they are too small to determine their morphology or crystallography from the images. In order to determine the Burger's vector, detailed analysis with different diffraction vector **g** is desired.

Others [8,21] have seen no evidence of fine precipitation in 316 type stainless steels after neutron irradiation at 55–250°C at doses of >1–2 dpa in the HFIR. The present irradiation at 90°C and 250°C, however, induced a low number density of particles, identified as $M_{23}C_6$ from a spacing of the Moiré fringe and/or diffraction pattern. They occurred in the matrix but not on grain boundaries. $M_{23}C_6$ is a radiation-retarded thermal phase, but when radiation-induced solute segregation (RIS) is suppressed at low radiation temperature, the phase could be enhanced during neutron irradiation [8].

4.2. Relation between microstructures and mechanical properties

Load–elongation curves for the SS-3 flat tensile specimens of 316LN irradiated in the same capsules and tested as part of this experiment are shown in Fig. 5(a) and (b), and the corresponding tensile data are shown in Table 4 Ref. [4]. The radiation-induced changes in

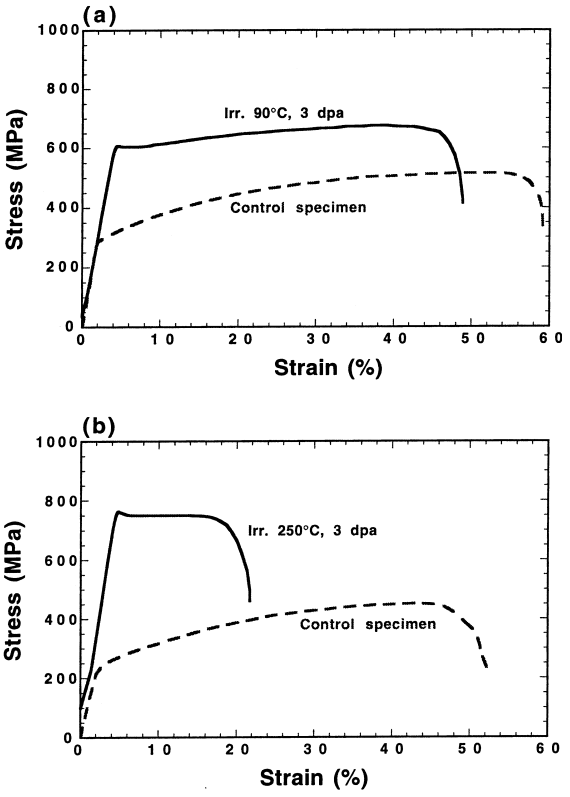

Fig. 5. Load–elongation curves for SS-3 tensile specimens of 316LN irradiated and tested at: (a) 90°C and (b) 250°C.

Table 4
Tensile properties of solution annealed 316LN

Dose (dpa)	Irr. temp. (°C)	Test temp. (°C)	YS (MPa)	UTS (MPa)	Eu (%)	Et (%)
0	–	25	298	582	62.0	68.5
0	–	90	285	516	50.2	57.2
0	–	250	214	451	40.8	51.3
2.9	83–101	90	610	674	37.7	45.0
2.9	83–101	90	605	677	37.0	46.1
3.0	250–300	250	760	764	11.7	18.8
3.0	250–300	250	724	735	12.7	20.8

tensile properties are more severe at 250°C than at 90°C. Irradiation at 90°C increased the yield strength from about 285 MPa up to about 600 MPa, and resulted in a modest reduction in both the strain hardening rate and the uniform elongation. A larger increase in yield strength occurred for the irradiation at 250°C. Following an initial yield drop, the engineering stress to the onset of necking exceeded 10%. These data are plotted in Fig. 6(a) and the corresponding number density data for dislocation loops, black dots and precipitates are shown in Fig. 6(b). While the density of precipitates is nearly constant, the density of dislocation loops and black dots increase and decrease, respectively, with irradiation temperature.

According to the theory of dispersed barrier hardening [22,23], an increase in yield stress, $\Delta\sigma_y$, is related to the increase in applied stress required to move a dislocation through a field of obstacles of strength α such that

$$\Delta\sigma_y = M\alpha\mu b(Nd)^{1/2}, \quad (1)$$

where M, α, μ, b, N and d are the Taylor [22] factor, barrier strength of obstacles, the shear modulus of the matrix, the Burger's vector of moving dislocation, the density of obstacles and the mean diameter of obstacles, respectively. In the present study, perfect loops and precipitates have only a small effect on the increase in applied stress due to their small number densities, and are therefore neglected in this calculation. Assuming the obstacles to be Frank loops and black dots, their contributions to hardening are as follows:

$$(\Delta\sigma_y)^2 = (\Delta\sigma_{\text{Frank loop}})^2 + (\Delta\sigma_{\text{Black dot}})^2. \quad (2)$$

With a Taylor factor of 3.06 [24], a shear modulus of 58×10^3 MPa and a value of $\alpha_{\text{Black dot}} = 0.146$ [25], values of $\alpha_{\text{Frank loop}} = 0.5$ was obtained for 90°C and 250°C. This value is in good agreement with the data of Odette and Frey [26] and of Garner et al. [27] and is much lower than the Orowan value for impenetrable obstacles, indicating that these defects may be sheared or assimilated by mobile dislocations during deformation. The presence of shearable obstacles is consistent with the observed decrease in strain hardening capacity in austenitic stainless steel irradiated at 90°C and 250°C. Although the number densities of defect clusters

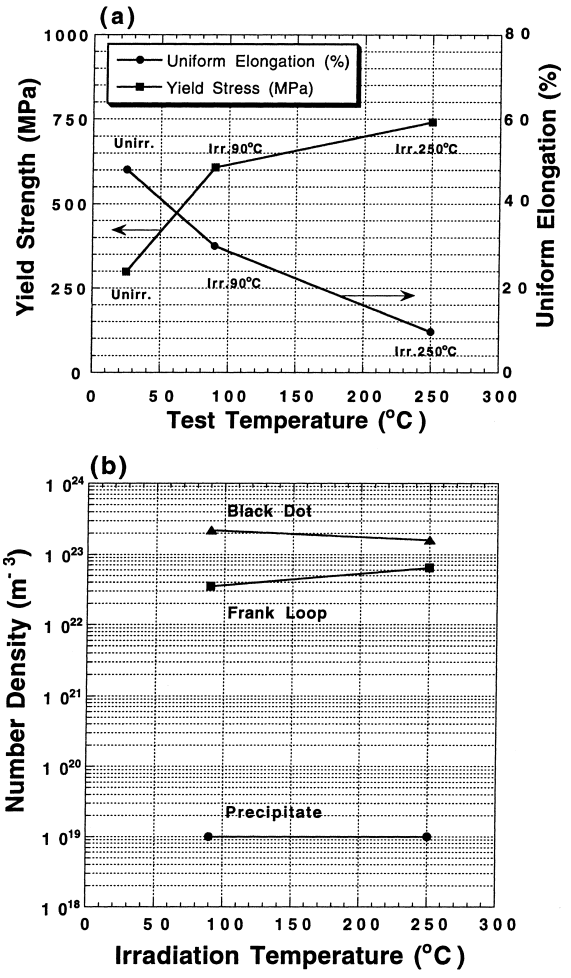

Fig. 6. Dependence of: (a) the yield strength and the uniform elongation, and (b) the dislocation loop density, the black dot density and the precipitate density on irradiation temperature.

and Frank loops change only slightly between 90°C and 250°C, there is significantly less strain hardening capacity at the higher temperature. This suggests that there is a tendency for dislocation channeling to occur at 250°C and for deformation to be more homogeneous at 90°C.

The relationships between the loop microstructure and dislocation channeling have been discussed recently [28], and a detailed model of the intersection and elimination of Frank loops by glide has been proposed [29]. We suggest that the increased hardening and more severe loss of strain-hardening capacity (SHC) observed here at 250°C compared to 90°C (Fig. 5) are related to the dislocation channeling and the increased number density of Frank loops developed at the higher temperature and the deformation to be more homogeneous at the lower temperature.

5. Conclusions

Specimens of an annealed austenitic stainless steel 316LN irradiated at about 90°C and about 250°C have been investigated by transmission electron microscopy. The irradiations introduced Frank loops and black dots, and a low density of radiation-enhanced precipitates in the matrix. Additionally, at 250°C, some unfaulted loops were seen. By expressing the yield strength change as due to Frank loops and black dots, the barrier strengths of Frank loops at 90°C or 250°C was determined to be 0.5. This represents reasonable values for the barrier strength of small obstacles in neutron-irradiated austenitic stainless steels. The presence of shearable obstacles, especially faulted loops which have the higher barrier strength, is consistent with the observed decrease in strain hardening capacity in austenitic stainless steel irradiated at 90°C and 250°C. Although the number densities of defect clusters and Frank loops change only slightly between 90°C and 250°C, there is significantly less strain hardening capacity at the higher temperature. This suggests that there is a tendency for dislocation channeling to occur at 250°C and for deformation to be more homogeneous at 90°C.

Acknowledgements

The authors are grateful to Dr M.L. Grossbeck for providing valuable irradiated samples. They also would like to thank Drs A.F. Rowcliffe, R.E. Stoller, S.J. Zinkle, and J. Bentley for their helpful discussions and assistance in TEM observation. This research was supported in part by an appointment to the Oak Ridge National Laboratory Postdoctoral Research Associates Program administered jointly by the Oak Ridge Institute for Science and Education and Oak Ridge National Laboratory.

References

[1] A.F. Rowcliffe, ITER Material Assessment Report for Stainless Steels, ITER Doc. G A1 DDD 1 97-12-08 W 0.2, December 1997.
[2] J.E. Pawel, A.F. Rowcliffe, D.J. Alexander, M.L. Grossbeck, K. Shiba, J. Nucl. Mater. 233–237 (1996) 202.
[3] G.E. Lucas, J. Nucl. Mater. 206 (1993) 287.
[4] D.J. Alexander, J.E. Pawel, M.L. Grossbeck, A.F. Rowcliffe, K. Shiba, Fusion Reactor Materials Semiannual Report for Period Ending 31 December 1995, DOE/ER-0313/19 (1996) 204.
[5] A.W. Longest, D.W. Heatherly, K.R. Thoms, J.E. Corum, Fusion Reactor Materials Semiannual Report for Period Ending 31 March 1991, DOE/ER-0313/10 (1991) 3.
[6] A.W. Longest, D.W. Heatherly, J.E. Wolfer, K.R. Thoms, and J.E. Corum, Fusion Reactor Materials Semiannual Report for Period Ending 30 September 1991, DOE/ER-0313/11 (1992) 30.
[7] A.W. Longest, D.W. Heatherly, K.R. Thoms, J.E. Corum, Fusion Reactor Materials Semiannual Report for Period Ending 31 March 1992, DOE/ER-0313/12 (1992) 24.
[8] S.J. Zinkle, P.J. Maziasz, R.E. Stoller, J. Nucl. Mater. 206 (1993) 266.
[9] M. Kiritani, Ultramicroscopy 39 (1991) 135.
[10] P.J. Maziasz, C.J. McHargue, Int. Mater. Rev. 32 (1992) 190.
[11] J.W. Corbett, Electron Radiation Damage in Semiconductors and Metals, Solid State Physics, suppl. 7, Academic Press, New York, 1966.
[12] W. Schilling, P. Ehrhart, K. Sonnenberg, in: M.T. Robinson, F.W. Young Jr. (Eds.), Fundamental Aspects of Radiation Damage in Metals, vol. 1, CONF-751006-P1, NTIS, Springfield, VA, 1975, p. 470.
[13] P.J. Maziasz, J. Nucl. Mater. 205 (1993) 118.
[14] M.P. Tanaka, P.J. Maziasz, A. Hishinuma, S. Hamada, J. Nucl. Mater. 141–143 (1986) 943.
[15] M. Horiki, M. Kiritani, J. Nucl. Mater. 212–215 (1994) 246.
[16] H.R. Brager, J.L. Straalsund, J. Nucl. Mater. 46 (1973) 134.
[17] P.J. Barton, B.L. Eyre, D.A. Stow, J. Nucl. Mater. 67 (1977) 181.
[18] P.J. Maziasz, Effect of He Content on Microstructural Development in Type 316 Stainless Steel under Neutron Irradiation, ORNL-6121, Oak Ridge National Laboratory, Oak Ridge, TN 37831, 1985.
[19] H.R. Brager, F.A. Garner, E.R. Gilbert, J.E. Flinn, W.G. Wolfer, in: M.L. Bleiberg, J.W. Bennet (Eds.), Radiation Effects in Breeder Reactor Structural Materials, TMS-AIME, New York, 1977, p. 727.
[20] S.J. Zinkle, J. Nucl. Mater. 150 (1987) 140.
[21] P.J. Maziasz, Am. Nucl. Soc. Trans. 39 (1981) 433.
[22] U.F. Kocks, Metall. Trans. 1 (1970) 1121.
[23] P.M. Kelly, Int. Metal. Rev. 18 (1973) 31.
[24] H.R. Higgy, F.H. Hammad, J. Nucl. Mater. 55 (1975) 177.
[25] R.L. Sindelar, Reactor Materials Program – Microstructural and Mechanical Response of Types 304, 304L, and

308 Stainless Steels to low temperature Neutron Irradiation (U), WSRC-TR-93-196, June 1993.
[26] G.R. Odette, G. Frey, J. Nucl. Mater. 85/86 (1979) 817.
[27] F.A. Garner, M. Hamilton, N. Panayotou, G. Johnson, J. Nucl. Mater. 103/104 (1981) 803.
[28] S.M. Bruemmer, J.I. Cole, R.D. Carter, G.S. Was, Mater. Res. Soc. Symp. Proc. 439 (1997) 437.
[29] S.G. Song, J.I. Cole, S.M. Bruemmer, Acta Mater. 45 (1997) 501.